NOVEL FRACTAL ANTENNA ARRAYS FOR SATELLITE NETWORKS: CIRCULAR RING SIERPINSKI CARPET ARRAYS OPTIMIZED BY GENETIC ALGORITHMS

K. Siakavara

Radiocommunications Laboratory
Department of Physics
Aristotle University of Thessaloniki
54124 Thessaloniki, Greece

Abstract—A novel fractal antenna-array type is proposed. The design is based on the Sierpinski rectangular carpet concept. However, the generator is a circular ring area, filled with radiating elements, so the higher stages of the fractal development produce large arrays of circular rings which, besides the high directivity, have the advantage of the almost uniform azimuthal radiation pattern, attribute that many applications require. The introduced arrays can operate as direct radiating multi-beam phased arrays and meet the requirements of satellite communications links: high End of Coverage (EOC) directivity, low Side Lobe Level (SLL) and high Career to Interference ratio (C/I). These operational indices were further optimized by a synthesized multi-objective and multi-dimensional Genetic Algorithm (GA) which, additionally, gave arrays no more than 120 elements.

1. INTRODUCTION

The inspired combination of fractal geometry with the electromagnetic theory has led to the development of an innovative class of antennas, the fractal antennas. The fractal antenna engineering research is focused on two basic areas: the first deals with the analysis and design of fractal radiating elements, and the second concern the application of the fractal theory and the design of antenna arrays [1–3]. Both antenna types have attributes highly desirable in military as well as in commercial sectors. The fractal antenna elements, the majority of them being printed configurations, have compact size, low profile and cost, multi-band operation, easy feeding and, potentially, optimized

---

Corresponding author: K. Siakavara (skv@auth.gr).

operation by suitable modification [4–9]. On the other hand, the application of the fractal technique to the design of an antenna array can produce radiating systems of large size, and as a consequence of high gain, frequency-independent or multi-band characteristics and radiation patterns with low side-lobe level [1–3, 10]. Moreover, they can be fed one by one, thus operating as Direct Radiating Antennas (DRAs) and can function as phased arrays without the disadvantages of the classical systems of Focal Array Fed Reflectors (FAFRs) used in the past. Due to these benefits a fractal array could be candidate to serve a modern satellite communication network, for these systems need large antennas, which illuminate the area under coverage with overlapped beam spots with high Maximum and End of Coverage Directivity (D_{EOC}), high Carrier to Interference (C/I) ratio and low Side Lobe Level (SLL). For all that, the required high directivity can be obtained by antennas with large size, and this fact involves large number of elements and potentially large inter-element distances. So, the designers face two problems a) the grating lobes that inevitably come from the large distance between the elements, and b) the complexity as well as the high cost of the system due to the large number of the elements that necessitate large number of phase shifters and various modules.

Methods to confront the above problems have been proposed. A widely used technique is to separate the array in sub-arrays, fed by properly weighted excitations [11, 12]. Innovative techniques, based on the architecture of the arrays, that effectively solve both the problems of grating lobes and the large number of control points have been recently proposed: a) the sparse arrays synthesized by uniformly excited elements located onto a non-regular grid and b) the thinned arrays that are produced from initial regular arrays by properly withdrawing a certain number of elements. All the modifications imposed on the arrays are done via stochastic or deterministic procedures [13–22]. Moreover, combination of the above concepts have led to evolutionary methods, which by arranging the array elements in thin-aperiodic lattices have dealt with the problems successfully [23–27].

The fractal technique has been proposed as a separate alternative technique for the design of a DRA configuration that meets the requirements of low side lobes and small number of control points. The fractal technique competes with the other methods because it permits to realize arrays with very small number of elements, as can be combined with a) the thinning procedure [28] b) the genetic algorithms [29] or c) the method of clustering the array in sub-arrays with non-uniform excitation [30].

In conclusion, the innovative design techniques, deterministic or not, give solutions to one of the most serious problems of satellite antenna arrays, namely to control the SLL of their radiation patterns. In some cases the design methods, followed by an optimization technique, can lead also to an efficient control of the Carrier to Interference ratio. Almost all the proposed configurations suffer from the disadvantage of the large number of elements and the complexity of the feeding network. The target of the present work was to synthesize satellite direct radiating array configurations which besides the attributes of the low side lobes and the large C/I, would have elements, the number of which will be not greater than some tens and that would need a simple feeding network. The synthesis of the proposed arrays is based on the rectangular Sierpinski carpet concept. However, it is realized by a novel configuration made up of circular rings. The first and second stages of growth are studied. Both stages lead to operational characteristics that meet the requirements of a satellite coverage. The drawback of the array of the second stage is the large number of elements that makes it non-competitive to other types of large antennas. On the contrary, the first stage produces an array with small number of elements and a geometry that is susceptible to improvement, in order the features of the radiation pattern to be further optimized. For the optimization, a genetic algorithm process was chosen. Due to the nature of the problem, namely the number of the objectives that had to be optimized and the number of the parameters, a specific genetic algorithm (GA) was synthesized and could be classified in the category of Multi-Objective and Multi-Dimensional GAs.

2. THE CIRCULAR RING SIERPINSKI-CARPET FRACTAL ARRAY

The fractal technique is based on the idea of realizing the radiation characteristics by repeating a structure in arbitrary or regular scales. The basic scheme of a fractaly designed radiating system is a generating sub-array. In particular, the entire array can be formed recursively through repetitive application of the generating sub-array under a specified scaling factor which is one of the parameters of the problem. This process is realized following potentially two different strategies: By one of them, the repetition of the generating sub-array is made in such a way that the size and number of the elements of the array get larger from stage to stage. So, at the nth stage, the size of the array is equal to the size of the generating sub-array multiplied by the nth power of the scaling factor, and the elements' population is the

$(n + 1)$th power of the number of elements of generating array. By the second strategy, the entire area, which the final array is permitted to occupy, is defined a priori. Then, by the process of the proper repetition of the generator, the available area is filled by scaled replicas of the generator. In this case solely the number of the elements of the array becomes larger from stage to stage, whereas the total size of the array does not change. The Sierpinski fractal arrays belong to this type of fractal configurations.

The Sierpinski rectangular carpet and triangular gasket have been efficiently used in the past for the realization of antenna arrays with specific operational features [1, 2, 31]. Both of these types, although can produce arrays with high directivity and potentially low side-lobes, cannot give radiation patterns with azimuthal uniformity. In the present work a novel approach is introduced: following the Sierpinski concept, however with another shape of generator. The geometry, which would fulfill the requirement of azimuthally uniform radiation pattern, is the circular ring, and this shape was used as generator.

2.1. The Array Synthesis

The novel array, in accordance to the rectangular carpet concept, is developed as follows: To define the correspondence between the rectangular carpet and the proposed array, suppose that the permissible area for the rectangle array has size $L_t \times L_t$. The configuration of the generator is shown in Fig. 1(a). The shadowed area represents the region in which the radiating antenna elements could be positioned whatever shape or size would have. The remaining rectangular white sub-areas are empty of elements or have elements that are turned off. Equivalently, the entirely available area for the novel array would be a circular disc of radius R_t (Fig. 1(b)). The shadowed area, in this configuration instead of a rectangle, would be a circular ring of width w_o. If we consider that the internal radius is r_o, the width w_o is defined as $w_o = \frac{R_t - r_o}{3}$. This definition is in agreement with the rectangular carpet in which $L_S = \frac{L_t}{3}$. The remaining area is divided in rings of width equal to w_o as shown in Fig. 1(b). These rings are empty or have antennas that are turned off whereas, the central ring is full of radiating elements.

Figures 2(a) and 2(b) depict the first stage of fractal development of the rectangular and circular ring carpet. In the circular ring case, each one of the rings is divided in three sub-rings of equal width, $w_1 = \frac{w_o}{3}$. So, a total of three blocks, each one with three rings, is formed, and the number of all the rings is $N_{r2} = 3^2$. All three sub-rings of the block around the center of the array are filled with
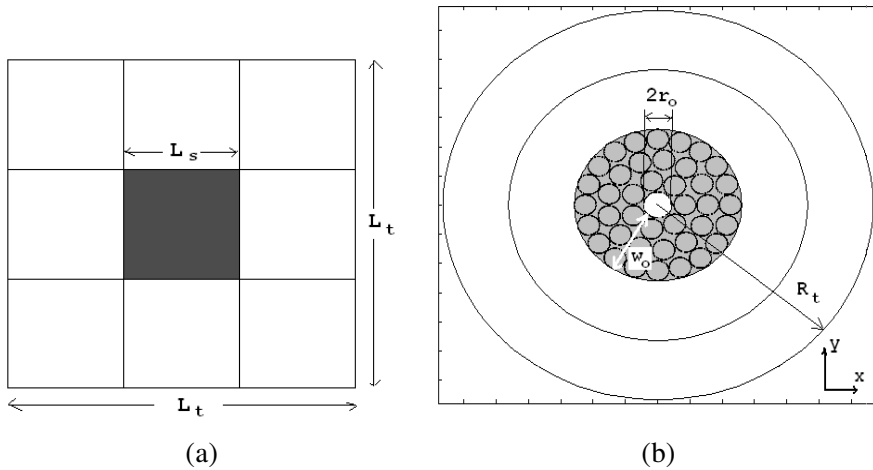
Figure 1. The generator subarray (a) rectangular, (b) circular ring, filled with antenna elements.

antenna elements which are turned on. These elements would be circular apertures or have another shape. In the present work the circular aperture was chosen. In accordance to the Sierpinski concept the central sub-rings of the other two blocks are filled with radiating elements whereas the remaining sub-rings have turned-off elements or are empty of antennas.

Following the same procedure, the second stage of fractal development is produced (Fig. 3(c)). In the circular ring fractal array, each of the sub-rings of the previous stage is also divided into three rings of equal width, which is $w_2 = \frac{w_1}{3} = \frac{w_o}{9}$. In this way, the array is formed by a total of nine blocks, each one having three rings of width w_2 and the total number of rings being $N_{r3} = 3^3$. The central three of N_{r3}, the 5th and 8th block areas are full of turned on antenna elements. In the 4th, 6th, 7th and 9th blocks, the central sub-ring is filled with elements that are turned on with size smaller than that of the other elements. The remaining area of the array is empty. So, the configuration of the second stage of growth has five rings with large and four rings with small elements.

In all antennas a unique element would be placed in the empty area around the center of the arrays. This placement is somehow arbitrary, is by the decision of the designer and would enhance the performance of the arrays a little.
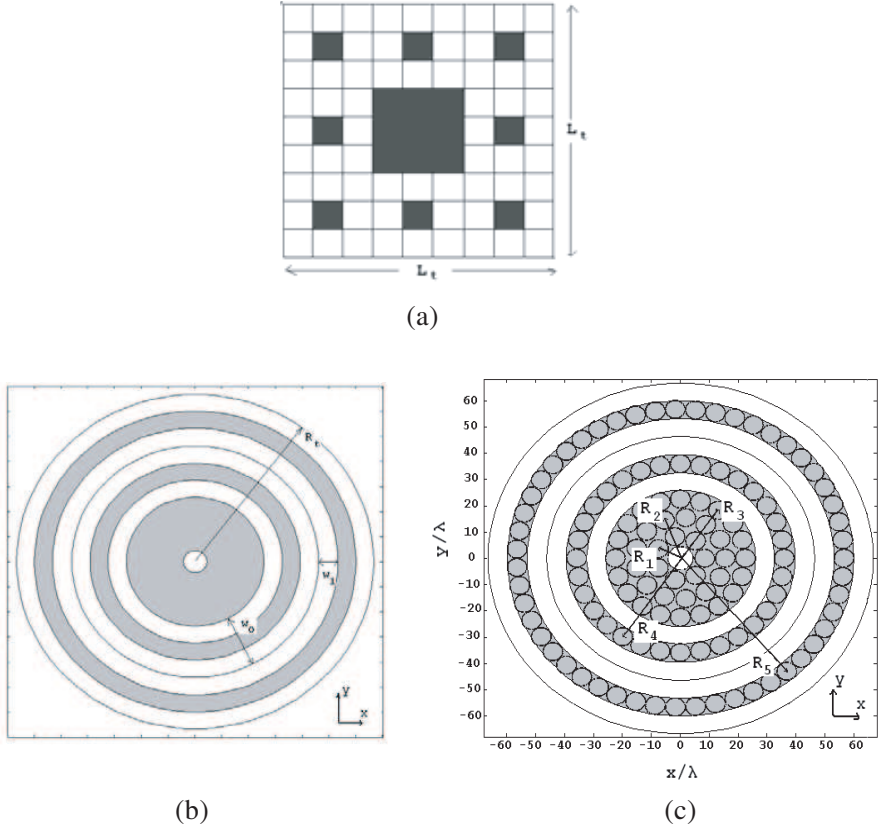
(a)

(b)   (c)

Figure 2. The geometry of the 1st stage of growth. (a) The rectangular configuration, (b) the circular configuration.

2.2. The Fields

The array factor and the total field of the first stage of growth (Fig. 2(c)), in accordance with the antenna array theory [32], are described by Equations (1) and (2) respectively,

$$AF1(\theta, \varphi) = I_o + \sum_{i=1}^{5} \sum_{j=1}^{N_i} I_{ij} e^{jkR_i \sin\theta \cos(\varphi - \varphi_{ij})} \tag{1}$$

$$E1_{tot}(\theta, \varphi) = AF1(\theta, \varphi) \cdot E_{el}(\theta, \varphi) \tag{2}$$

where R_i is the radius, and N_i is the number of elements of the ith ring. φ_{ij} and I_{ij} are, respectively, the location and excitation of the jth element on the ith ring, and the coefficient I_o is the excitation of the

(a)

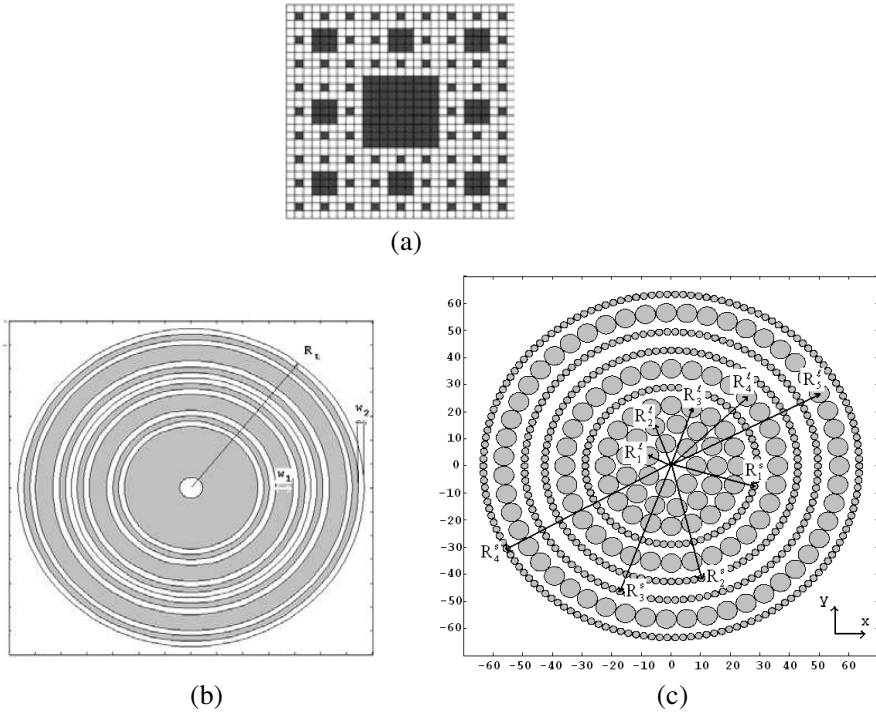(b)   (c)

Figure 3. The geometry of the 2nd stage of growth. (a) The rectangular configuration, (b) the circular configuration, (c) the circular ring areas filled with antenna elements.

element located at the center. $E_{el}(\theta,\varphi)$ is the field of each radiating element. If the central element has size different from the rest of the elements, the coefficient I_o is multiplied separately by the respective element field.

The total field for the second stage configuration (Fig. 3(c)) is calculated by Equation (3)

$$E2_{tot}(\theta,\varphi) \ = \ I_o \cdot E_{el}^{\circ}(\theta,\varphi) + \left(\sum_{i=1}^{5} \sum_{j=1}^{N_i^{\ell}} I_{ij}^{\ell} e^{jkR_i^{\ell}\sin\theta\cos\left(\varphi-\varphi_{ij}^{\ell}\right)} \right) \cdot E_{el}^{\ell}(\theta,\varphi)$$

$$+ \left(\sum_{i=1}^{4} \sum_{j=1}^{N_i^{s}} I_{ij}^{s} e^{jkR_{si}\sin\theta\cos\left(\varphi-\varphi_{ij}^{s}\right)} \right) \cdot E_{el}^{s}(\theta,\varphi) \qquad (3)$$

In the above equation, the terms of the total summation are divided in three groups depending on the size of the antenna elements:

the central element with field $E_{el}^{\circ}(\theta, \varphi)$, the group of the elements with large size and field $E_{el}^{\ell}(\theta, \varphi)$ and the elements with small size and field $E_{el}^{s}(\theta, \varphi)$.

Both the above array schemes would serve, as mentioned previously, a satellite system. The common practice in these applications is to synthesize an antenna array having the proper size, configuration and excitation to produce narrow main beams of radiation that create on the earth spots of illumination which are overlapped and with very small angular width. Moreover, inside the terrestrial area under coverage there are spots that use the same frequency band, and the angular distance between them is very small. So, the possibility of interference is very high. The solution to this problem is given by the antenna array via suitable modification of its radiation pattern in order the radiation toward the co-channel spots to be minimized. Furthermore, another general requirement concerns the level of the radiation lobes appearing in the range out of coverage area — on earth as well as out of earth. This level must be as small as possible.

As an application example of the proposed design method, an array was synthesized with the requirement to produce on the earth spots with $0.65°$ angular width and to cover, via overlapped spots, an almost circular area with angular width $2 \cdot 1.445°$. The first step of the design is to select the radius R_t of the entire array. The larger it is, the larger would be the directivity, but there is a tradeoff between this quantity and the size available for satellite antennas. Furthermore, a very large antenna will have undesirably large number of elements. If we approximately consider the entire array as a circular uniformly excited aperture, the radius R_t, in wavelengths, and the half-power beam-width $HP°$ are related with the equation $R_t \simeq 29/HP°$ [29]. For $HP° = 0.65°$, $R_t \simeq 45\lambda$. However, the circular ring fractal arrays have no uniform excitation because there are empty areas and elements with different sizes. So, a larger radius is necessary. Some calculations of the radiated field proved that in order the directivity to exceed the value of $40\,\text{dB}$ a radius about 68λ was necessary. Following the procedure described above, the arrays of Figs. 2(c) and 3(c) were produced. The arithmetic values of their geometrical parameters are included in Table 1. In both cases the large elements of the array were suggested to be circular apertures of uniform excitation with radii $r_{el}^{\ell} = 3.4\lambda$, whereas the small elements are uniformly excited apertures with radii $r_{el}^{s} = 1.2\lambda$. At the center of both arrays a unique circular aperture, uniformly excited with radius $r_{el}^{\circ} = 4.4\lambda$, was located.

The directivity patterns of the arrays are computed by

Table 1. The geometry of the 1st stage (Fig. 2(c)) and the 2nd stage (Fig. 3(c)).

	1st stage	2nd stage			1st stage	2nd stage	
R_1	8.4λ	R_1^ℓ	8.4λ	N_1	7	N_1^ℓ	7
R_2	15.5λ	R_2^ℓ	15.5λ	N_2	13	N_2^ℓ	13
R_3	22.5λ	R_3^ℓ	22.5λ	N_3	20	N_3^ℓ	20
R_4	35.9λ	R_4^ℓ	35.9λ	N_4	32	N_4^ℓ	32
R_5	56.6λ	R_5^ℓ	56.6λ	N_5	51	N_5^ℓ	51
		R_1^s	29λ	N_6		N_1^s	72
		R_2^s	42.7λ	N_7		N_2^s	104
		R_3^s	49.5λ	N_8		N_3^s	114
		R_4^s	64.3λ	N_9		N_4^s	150
				N_{total}	$123 + 1$		$563 + 1$

Equation (4a)

$$D\left(\theta, \varphi\right) = D_{\max} \left|E_{tot}(\theta, \varphi)\right|_{norm} \tag{4a}$$

where

$$D_{\max} = \frac{4\pi}{\int\limits_0^{2\pi} \int\limits_0^{\pi} \left(\left|E_{tot}(\theta, \varphi)\right|_{norm}\right)^2 \sin\theta d\theta d\varphi} \tag{4b}$$

and

$$\left|E_{tot}(\theta, \varphi)\right|_{norm} = \left|E_{tot}(\theta, \varphi)\right| / \left|E_{tot}(\theta_{\max}, \varphi_{\max})\right| \tag{4c}$$

The central beams of the above arrays and respective spots are at $\theta = 0°$. The radiation patterns of these beams are depicted in Figs. 4 and 5. The calculations were made via Equations (2) to (4), with MathCad software. In order to check the azimuthal uniformity of the patterns, φ-cuts from 0° to 90° per one degree were calculated. All the elements in both arrays were fed by currents of equal value, and the records of the arrays are presented in Table 2.

The End of Coverage Directivity (D_{EOC} [dBi]) is the directivity at $\theta = 0.65°/2$. For every spot a co-channel spot is located $2 * 0.56°$ apart, and it is required the radiation pattern to have a deep minimum in the range $0.795° \leq \theta \leq 1.445°$. This minimum is assessed by the quantity C/I, or more simple CI, defined as the ratio $D_{EOC}/(\max$

Table 2. The records of the initial circular ring Sierpinski carpets.

	$D_{\max}$ [dBi]	D_{EOC} [dBi]	CI [dB]	SLL [dB]
1st fractal stage	45	39.95	16.1	18.8
2nd fractal stage	44.95	37.18	7.18	21

level inside co-channel region). The range 'out of coverage-on earth' corresponds to angles θ between 1.445° and almost 8°. In this range as well as for $\theta > 8°$ the ratio of the peak level of directivity over the side lobe is termed as SLL. In most of the applications it has to be greater than 20 dB. The quantity CI [dB] and SLL [dB] are measured as shown in Fig. 4.

From the results, it is obvious that the array of the second stage is inferior to that of the first stage. It has much more elements and smaller D_{EOC}, CI and SLL. However, in practice, large values for all the indices, D_{EOC}, CI, SLL, are required. The performance of both arrays could be improved applying an optimization technique. The challenge is to try to optimize the array of the first stage
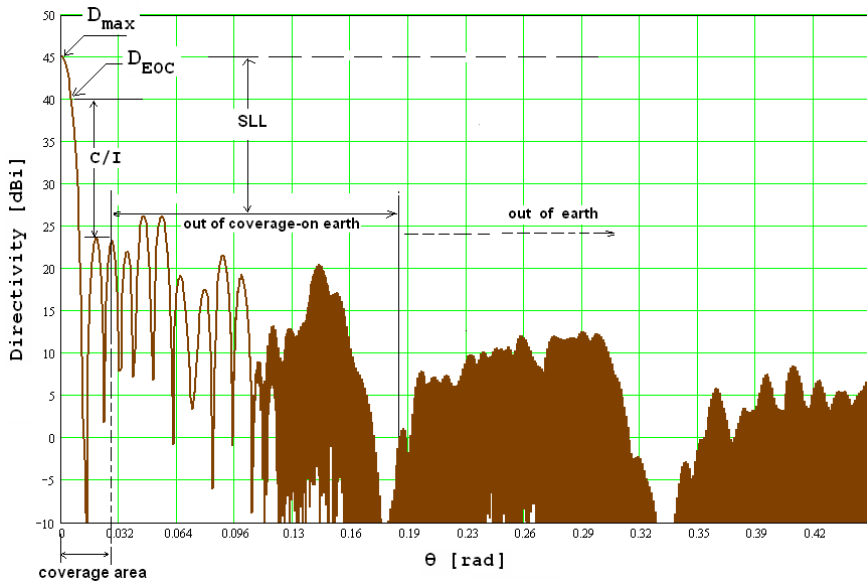

Figure 4. Patterns of the central beam of the array of the first stage of growth (Fig. 2(c)), φ-cuts from 0°–90°. All the elements are excited with equal currents.
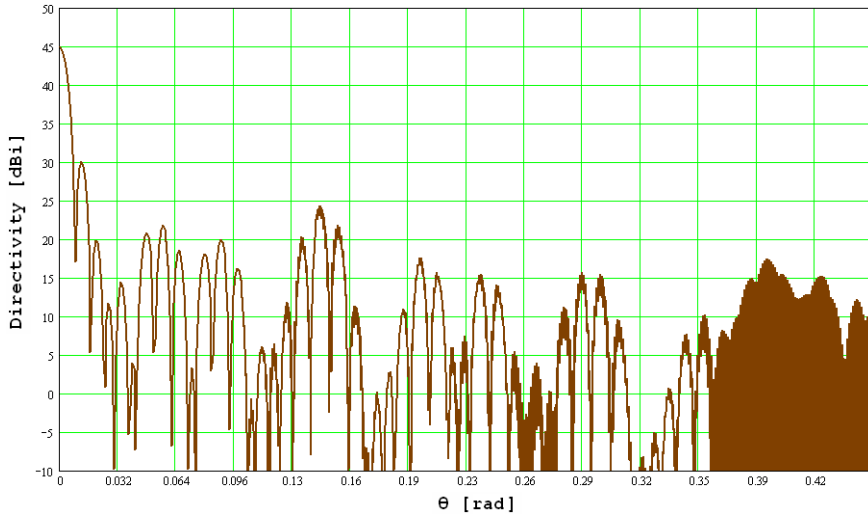
Figure 5. Patterns of the central beam of the array of the second stage of growth (Fig. 3(c)), φ-cuts from 0°–90°. All the elements are uniformly excited.

due to its small number of elements, and the target is, along with the improvement of the indices of operation, to further reduce the number of the elements. For the optimization, the GA method was selected, for reasons discussed in the following. The parameters that govern the performance of the array are the geometry and excitation. So, the target of the optimization procedure was to find a new configuration, coming from the initial one, as well as a suitable non-uniform excitation.

3. OPTIMIZATION BY GENETIC ALGORITHMS

Genetic Algorithms have been widely used in antenna synthesis and optimization problems [33, 34]. They have been proven efficient to finding the proper excitations or the suitable division of the arrays in sub-arrays in order the antenna to produce a desired radiation pattern with respect to the SLL and the directions of the nulls or to optimize the antenna by broadening the frequency bandwidth [11, 15–17, 33–35]. GAs have also been used to thin an array [18], in combination with Particle Swarm Optimization Technique to modify sparse arrays [21] or to modify fractal arrays [29, 36]. In all cases the target was the achievement of special performance features.

In the work at hand, a GA was produced to optimize the radiation features of the proposed circular ring Sierpinski carpet antenna array, in order to exhibit the features which are necessary for a satellite communication radiating system. The problem was complex, because the target was to modify the array in order to obtain the contemporaneous optimization of three quantities, the D_{EOC}, C/I and SLL. So, the problem was Multi-Objective. On the other side, the aim of the modification of the array was to find an optimum geometry and an optimum excitation. So, several parameters had to be optimized. This means that the optimization had to be multi-dimensional. These are the reasons for which a GA procedure was selected for the optimization: the GAs can deal with a large number of parameters and objectives. Moreover, in the problem at hand, there is a trade-off among the objectives. For example, the values of the parameters that ensure high D_{EOC} fail to give large C/I and SLL, and vice versa, or, satisfactory values could be obtained for D_{EOC} and SLL but not for the C/I. As a consequence, the problem would not have a unique solution, and a set of equally valid and alternative solutions is expected. It is an additional reason for which the GA procedure was selected for the specific problem: a GA has the potential of looking for more than one solutions in parallel.

3.1. Formulation

A general multi-objective and simultaneously multi-dimensional design problem can be expressed as the maximization of an objective vector

$$g(\bar{p}) = [g_1(\bar{p}), g_2(\bar{p}), \ldots, g_M(\bar{p})] \tag{5}$$

where $\bar{p} = [p_1, p_2, \ldots, p_N]$ is the vector, also termed chromosome, containing the parameters of the problem, and $g_i(\bar{p}), i = 1, \ldots, M$ are the objective functions termed cost functions. The objective vector represents the mapping between the search space and the space of the objectives. In the present problem the cost functions are three: the $D_{EOC}(\bar{p})$, $CI(\bar{p})$ and $SLL(\bar{p})$, and they are considered in the entire space out the coverage area. The radii R_3, R_4, R_5, (Fig. 2(c)), the numbers N_3, N_4, N_5 of the elements of the respective rings and the excitation were selected as the parameters which would maximize the cost functions. The strategy was to keep the radii R_1, R_2 unchanged because it is expected that high density of elements at the central area of the array would help the suppression of side lobes. It is also known that this attribute would be enhanced by non uniform excitation, namely by feeding the central elements of the array with currents larger than the currents of the rest elements. In the array under optimization, the elements of the rings with radii R_1, R_2, R_3,

R_4 were fed with current values P_o times the currents of the outer ring. The parameter P_o is the 7th parameter of the chromosome $\bar{p}$, which has the form

$$\bar{p} = [R_3, R_4, R_5, N_3, N_4, N_5, P_o] \qquad (6)$$

The multi-objective genetic procedure, in its classical approach, requires the maximization or minimization of the square mean value of the vector $g(\bar{p})$. In our case the maximization of this quantity does not ensure that all the objectives $D_{EOC}(\bar{p})$, $CI(\bar{p})$ and $SLL(\bar{p})$ will have contemporaneous satisfactory high values. So, in the synthesized algorithm these objectives worked as three separate cost functions. The ideal solution $\bar{p}$ would be the one that could simultaneously maximize all three cost functions, but due to the trade-off among them it seems rather impossible. Each cost function has its own cost surface as well as its own global maximum, but, possibly, these maxima would not correspond to the same chromosome $\bar{p}$. Moreover, the global maximum values of the objectives D_{EOC}, CI and SLL of the proposed array configuration are not known a priori.

So, the GA had to be synthesized in a way that would make it capable to explore the trade-offs of the objectives and to work as an unsupervised procedure, capable to converge not necessarily to a unique solution but to a set of optimal solutions of equal valid.

The code of the synthesized GA was realized with FORTRAN, keeps the attributes of a classical multi-objective algorithm, and is enhanced with elitist strategies and criterions that work as thresholds. All of them decide on how many and which of the individuals-chromosomes will pass from one generation to the next. The number of the chromosomes at the ith iteration-generation is termed as N_{pop}^i.

The GA includes the following steps:

Step 1: Generate an initial population of N_{pop}^1 chromosomes $\bar{p}$.

Step 2: Calculate the cost functions for all chromosomes, $D_{EOC}(\bar{p}^i)$, $CI(\bar{p}^i)$ and $SLL(\bar{p}^i)$, $i = 1, 2, \ldots, N_{pop}^1$

Step 3: Select $N_{mat}^i \leq N_{pop}^i$ individuals for mating. This number is one of the parameters of the algorithm. It is calculated as a fraction m_f of the population of the ith iteration, and it is the same for all the iterations. So, $N_{mat}^i = m_f \cdot N_{pop}^i$, where N_{pop}^i is the number of individuals in the ith generation. The selection of which of the chromosomes amongst the individuals of the ith population will constitute pairs to produce two offspring is made randomly.

Step 4: Execute the process of mating. The classical approach is to randomly select crossover points in the chromosomes of the parents and exchange the parameters. In the problem at hand this procedure could not introduce new information because each continuous parameter, which was randomly initialized in the first

population, is transferred to the next generation simply in different combinations. So, another technique was applied. The nth parameter, $p_{n,off}^i$, of the offspring, at the ith generation is produced by the linear combination of the respective parameters of its parents. The parameters of the first offspring are produced via the rule

$$p_{n1,off,}^i = \beta p_{n,mom}^i + (1 - \beta)p_{n,dad}^i \tag{7}$$

and of the second offspring by

$$p_{n2,off}^i = (1 - \beta)p_{n,mom}^i + \beta p_{n,dad}^i \tag{8}$$

where β is a random number in the interval $[0, 1]$, and $p_{n,mom}^i$, $p_{n,dad}^i$ are the nth parameters in the mother's and father's chromosomes.

Step 5: Calculate the three cost functions for each offspring, namely $D_{EOC}(\bar{p}_{off}^i)$, $CI(\bar{p}_{off}^i)$ and $SLL(\bar{p}_{off}^i)$.

Step 6: Impose the rules to select which of the individuals — chromosomes will survive and constitute the next generation. The target of this selection is to discard the chromosomes that potentially, during the mating, would produce offspring with degrade.

a. At first, an elitism criterion is imposed. The values of all the three cost functions produced by the offspring are compared with the respective of their parents. The offspring replace their parents and pass to the $(i + 1)$th generation by the rule,

$$\bar{p}_n^{i+1} = \begin{cases} \bar{p}_{n,off}^i & \text{if } \begin{array}{l} D_{EOC}(\bar{p}_{n,off}^i) \geq D_{EOC}(\bar{p}_{n,par}^i) \wedge CI(\bar{p}_{n,off}^i) \\ \geq CI(\bar{p}_{n,par}^i) \wedge SLL(\bar{p}_{n,off}^i) \geq SLL(\bar{p}_{n,par}^i) \end{array} \\ \bar{p}_{n,par}^i & \text{otherwise} \end{cases} \tag{9}$$

where $D_{EOC}(\bar{p}_{n,par}^i)$, $CI(\bar{p}_{n,par}^i)$ and $SLL(\bar{p}_{n,par}^i)$ are the values of the cost functions of the respective parents.

b. A threshold D_{EOCthr}^i, CI_{thr}^i and SLL_{thr}^i, for every cost value, is established, and if we define the populations of the ith and $(i+1)$th iterations as P_{pop}^i and P_{pop}^{i+1}, then

$$\forall\, n \in (1, 2, \ldots, N_{pop}^i), \quad \bar{p}_n^i \in \left(P_{pop}^i \cap P_{pop}^{i+1}\right)$$
$$\text{if } D_{EOC}(\bar{p}_n^i) \geq D_{EOCthr}^i \wedge CI(\bar{p}_n^i) \geq CI_{thr}^i \wedge SLL(\bar{p}_n^i) \geq SLL_{thr}^i \tag{10}$$

The thresholds are not constant. They increase, by a step, from one iteration to the next, starting from values selected to be equal to those of the initial array of the first stage of growth (Fig. 2(c)). In this way, the number of chromosomes in the populations gradually decreases, and better performers are included from generation to generation.

Step 7: As mentioned previously, the global maxima of each cost function are not known a priori and potentially could not be obtained by the same chromosome. So, the GA can stop when a final population

of N_{stop} individuals is found, provided that these individuals ensure large values for all three cost functions. The genetic procedure stops when $N_{pop}^i \leq N_{stop}$, else the process goes back to Step 3. The flowchart of the synthesized GA is shown in Fig. 6.

3.2. Results

The genetic procedure described above was applied to an initial population with $N_{pop}^1 = 720$ chromosomes $\bar{p}$, produced from the fractal array of the first stage of growth (Fig. 2(c)). This relatively large number was chosen in order the algorithm to sample the cost surfaces in more detail. The individuals of the initial population were created randomly, with respect to the parameters of the chromosomes under the single constraint, the number of the elements in the rings to be less or equal to the maximum permissible. By this constraint it was ensured that the elements do not overlap, whereas, by the random selection, chromosomes with small number of elements were included in the population, and in this way the potential to find the GA solutions with number of elements smaller than that of the initial array was provided.

Other parameters that affect the performance of the GA were the steps by which the thresholds were increased. The target of this increase, as mentioned before, was to reject, from one generation to the next, the most 'weak' chromosomes, in the sense of the capability to ensure large values of the cost functions. This evolution procedure had to be made by a proper rate. If it was too fast, the populations would decrease quickly, and this fact would reduce the capability of the GA to converge to solutions that provide satisfactory high values of cost functions. On the other hand, a slow process would potentially lead to bad performers, the chance to contribute their traits to the next generation, degrading the capability of the algorithm to find good solutions. After many trials it was found that the best results are obtained with steps 0.05 dBi for the D_{EOC}, 0.15 dB for the CI and 0.1 dB for the SLL.

To keep track of the evolution of the generations, the number of the chromosomes and mean values $D_{EOC/mean}^i$, CI_{mean}^i and SLL_{mean}^i calculated on all chromosomes of the ith generation were found and stored. The results are depicted in Figs. 7(a) to 7(d), as a function of the order of generation and for various values of the parameter m_f.

In Figs. 7(a)–7(d), it is shown that each of $D_{EOC/mean}^i$, CI_{mean}^i and SLL_{mean}^i tends to a maximum value but not for the same value of m_f. This fact is a result of the tradeoff among the cost functions. It has to be pointed out that the mean values were a criterion to judge if
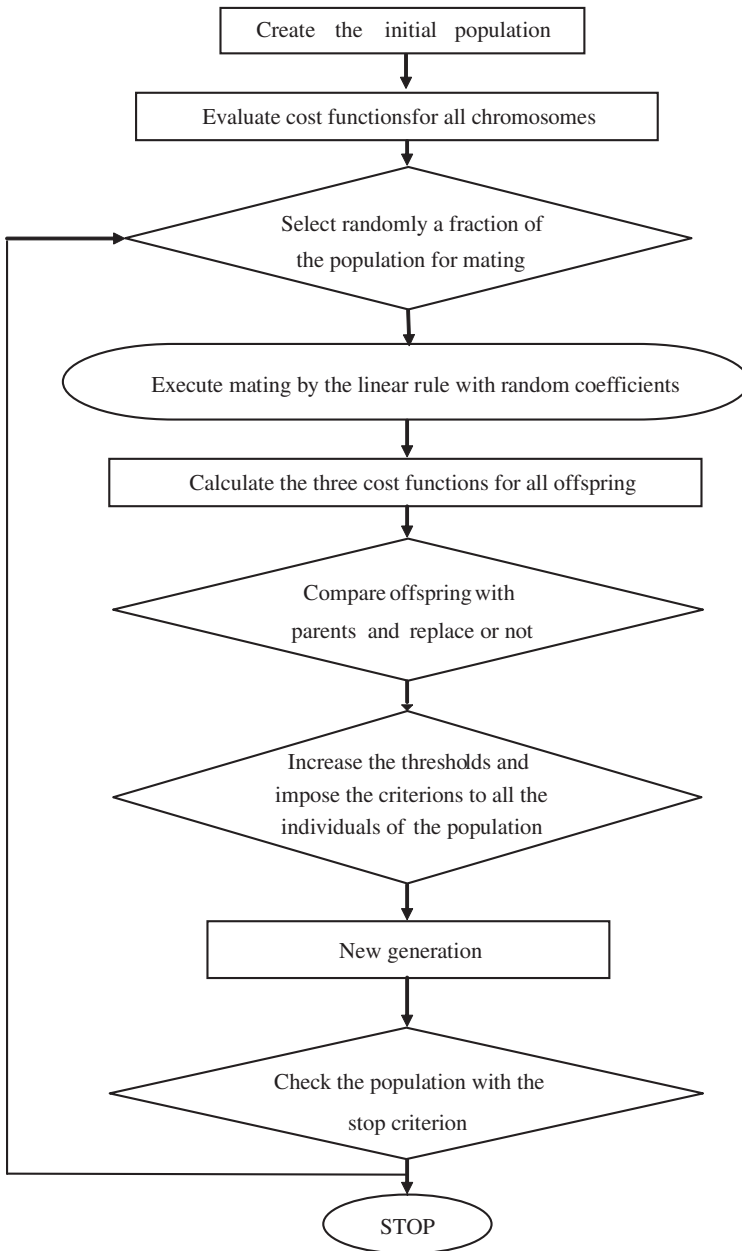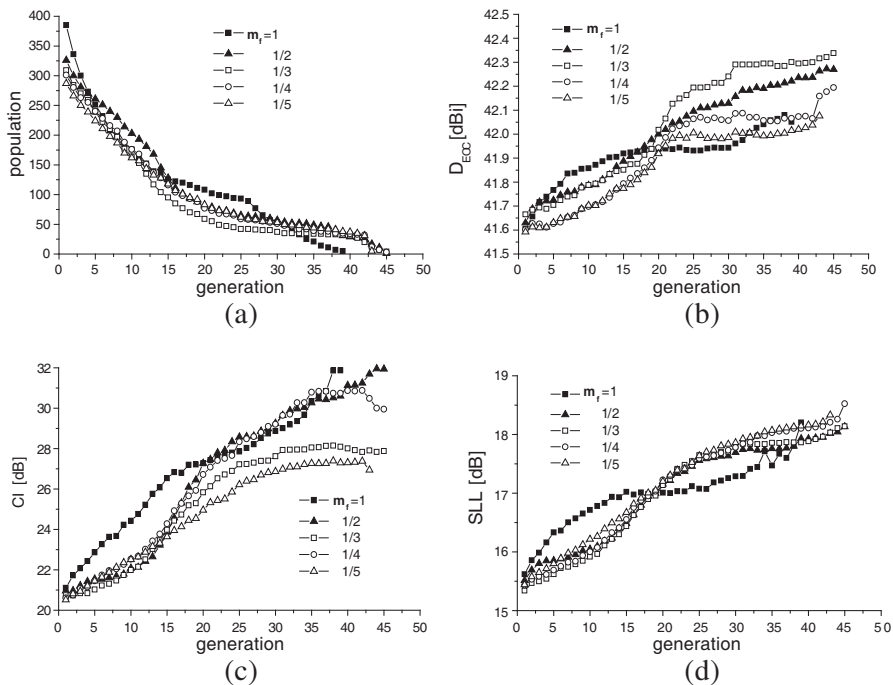
Figure 6. The GA process.

Figure 7. Results as function of the order of generation. (a) Number of individuals, (b) mean values of the End of Coverage Directivity, (c) mean values of the Carrier to Interference ratio, and (d) mean values of the SLL.

the generations tend to a better performance. So, independent of the mean values that would be larger or smaller, depending on the value of m_f, in the final population, and for every m_f, chromosomes, which ensure large values for all three cost functions, appear. Representative results, considered as the best, are included in Table 3.

Comparing the results of Tables 2 and 3, the general ascertainment is that the GA obtained to give solutions with total number of elements smaller than that of the initial array, D_{EOC} greater, at least 2 dB, CI greater, at least 11 dB, and SLL greater, at least 3 dB, than those of the initial array. It is observed that the solutions with a little larger D_{EOC} have smaller CI and SLL and vice-versa. Furthermore, for the smaller values of m_f the GA converges to solutions with larger number of elements, a little smaller values of SLL and significantly smaller values of CI. The size of all the arrays is $\sim 2R_5$, almost similar in all solutions. The large values of m_f, namely the strategy to mate the

most or all the individuals of each generation, allows the algorithm to converge with smaller number of iterations, as shown in Fig. 6(a), and also to search for and find solutions with better characteristics.

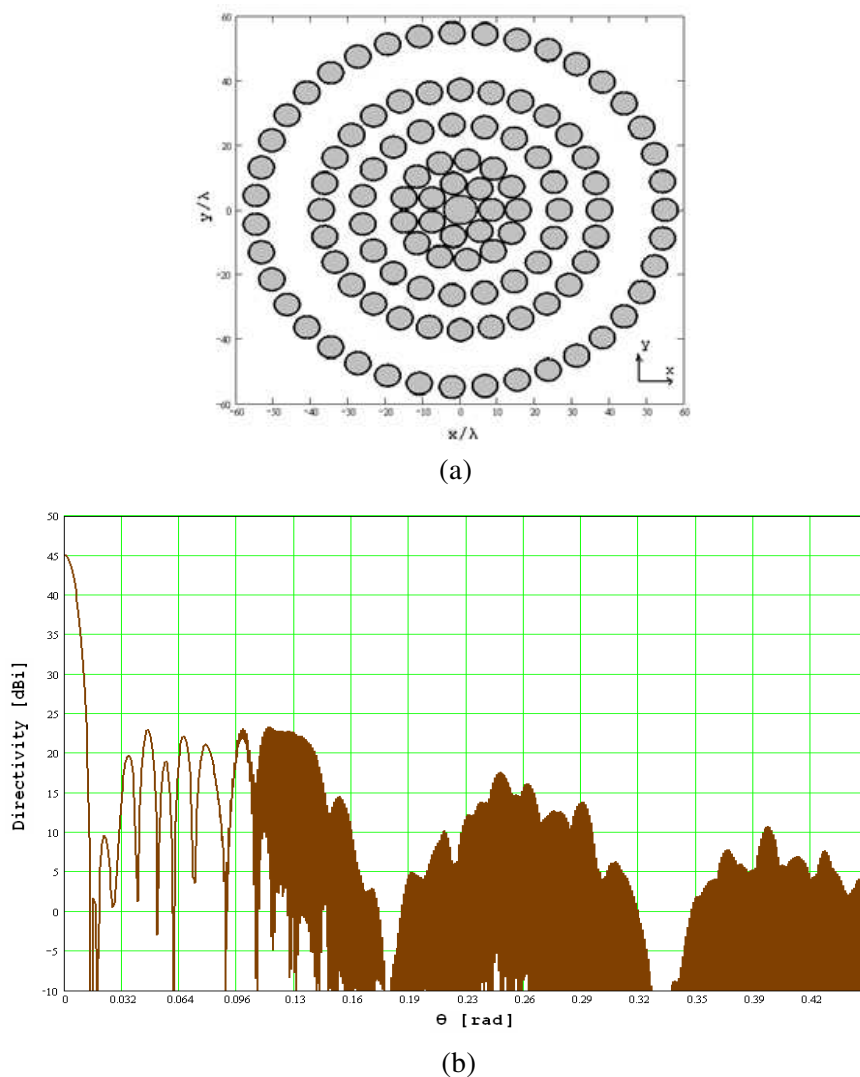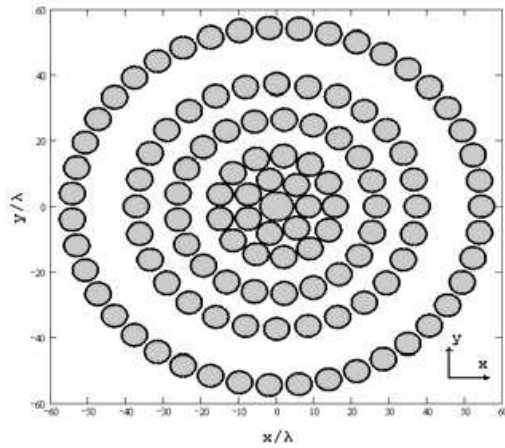The first two solutions of Table 3 could be considered as the best of

(a)
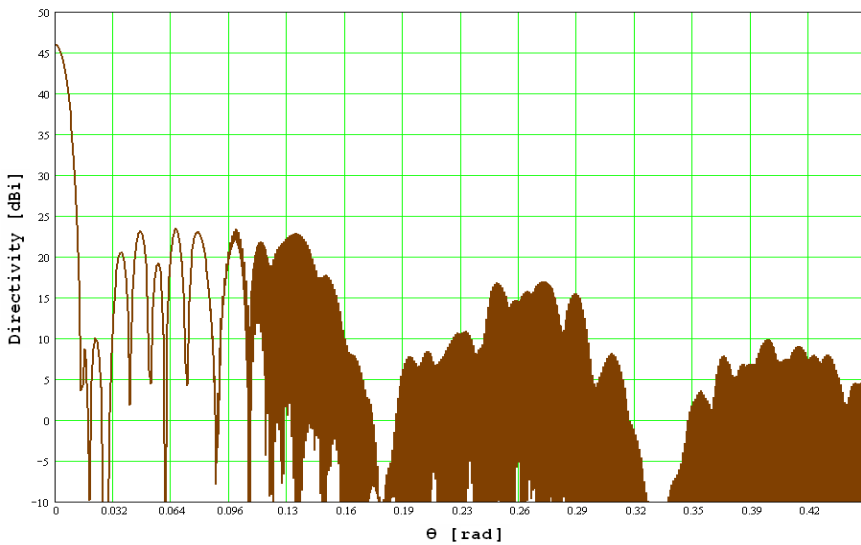

(b)

Figure 8. Solution 1: (a) The layout, outer radius 54.91λ, 107 elements. (b) Patterns of the central beam φ-cuts from $0°$–$90°$. $D_{EOC} = 42.04\,\mathrm{dBi}$, $CI = 32.07\,\mathrm{dB}$, $SLL = 21.78\,\mathrm{dB}$.

(a)

(b)

Figure 9. Solution 2: (a) The layout, outer radius 54.423λ, 113 elements. (b) Patterns of the central beam φ-cuts from $0°$–$90°$. $D_{EOC} = 42.21\,\text{dBi}$, $CI = 32.25\,\text{dB}$, $SLL = 22.59\,\text{dB}$.

all. The details of their geometry are presented in Table 4. The layouts and radiation patterns are depicted in Figs. 8 and 9. The calculations were made by applying the parameter values resulted from the GA, Equations (2)–(4) and MathCad software.

Table 3. The best solutions resulted from the GA.

solution	m_f	D_{EOC} [dBi]	CI [dB]	SLL [dB]	Total number of elements	R_5/λ	P_o
1	1	42.04	32.07	21.78	107	54.91	2
2	1	42.21	32.25	22.59	113	54.42	2
3	1/2	42.27	31.94	21.83	118	55.05	2
4	1/3	42.3	29	21.82	120	54.65	2
5	1/4	42.56	27.32	21.91	128	55.00	2
6	1/5	42.56	27.32	21.92	128	55.00	2

Table 4. The geometry of the first two solutions of Table 3.

	Solution 2	Solution 1			Solution 2	Solution 1
R_1	8.4λ	8.4λ		N_1	7	7
R_2	15.5λ	15.5λ		N_2	13	13
R_3	26.535λ	26.475λ		N_3	21	19
R_4	37.313λ	37.257λ		N_4	28	28
R_5	54.423λ	54.91λ		N_5	43	39
				N_{total}	$112 + 1$	$106 + 1$

4. CONCLUSIONS

The paper presents a novel process for the design of fractal large antenna arrays. The process is based on the rectangular Sierpinski carpet concept but starts from circular ring generator, and as a consequence the higher stages of fractal growth are arrays of circular ring areas filled with radiating elements. The benefits of the proposed antenna are a) the azimuthal uniformity of the radiation pattern, due to the circular configuration of the array b) the high directivity which is obtained with relatively small number of elements at the first stage of fractal development and c) the elements can be fed one by one, thus the system operates as a direct radiating and potentially phased array. These features would make the proposed arrays a good choice for a satellite communication platform. However, in these applications additional operational features are required: a) side lobe levels, very low compared to the peak values of the radiation b) high career to interference ratio in the co-channel areas of the network and c) radiating systems with small number of elements and low feeding complexity. What makes the design more difficult is that the

co-channel areas are located in a very small angular distance. An additional advantage of the proposed arrays, especially that of the 1st stage of growth, is the capability of improvement and, in this way, meeting the above requirements. A hybrid multi-objective and multi-dimensional Genetic Algorithm was synthesized for the optimization of the array of the first stage of growth. The algorithm, due to the nature of the problem, does not converge to a unique solution which would be the globally best one, but to a number of satisfactory solutions of equal valid. The genetic procedure is obtained to improve the operational features of the antennas. It increased a) the end of coverage directivity at least 2 dB b) the carrier to interference ratio at least 11 dB and c) the difference between the peak radiation and the level of side lobes at least 3 dB, and besides these improvements, gave arrays of no more than 120 elements.

REFERENCES

1. Werner, D. H., R. L. Haupt, and P. L. Werner, "Fractal antenna engineering: The theory and design of fractal antenna arrays," *IEEE Antennas and Propagation Magazine*, Vol. 41, No. 5, 37–59, 1999.

2. Werner, D. H. and S. Ganguly, "An overview of fractal antenna engineering research," *IEEE Antennas and Propagation Magazine*, Vol. 45, No. 1, 38–57, 2003.

3. Werner, H. and R. Mittra, *Frontiers in Electromagnetics*, IEEE Press, New York, 2000.

4. Siakavara, K. and F. Tsaldaris, "A multi-wideband microstrip antenna designed by the square curve fractal technique," *Microwave and Optical Technology Letters*, Vol. 41, No. 3, 180–185, 2004.

5. Siakavara, K., "Enhanced fractal microstrip antenna performance by using photonic bandgap fractal ground plane," *Microwave and Optical Technology Letters*, Vol. 42, No. 5, 397–402, 2004.

6. Siakavara, K. and T. Ganatsos, "Modification of the radiation patterns of higher order modes of triangular printed antennas by EBG ground planes," *IEEE Antennas and Wireless Propagation Letters*, Vol. 8, 124–128, 2009.

7. Salmasi, M. P., F. Hodjatkashani, and M. N. Azarmanesh, "A novel broadband fractal Sierpinski shaped, microstrip antenna," *Progress In Electromagnetics Research C*, Vol. 4, 179–190, 2008.

8. Azari, K. and J. Rowhani, "Ultra wideband fractal microstrip

antenna design," *Progress In Electromagnetics Research C*, Vol. 2, 7–12, 2008.

9. Cheng, H. R., X.-Q. Chen, L. Chen, and X.-W. Shi, "Design of a fractal dual-polarized aperture coupled microstrip antenna," *Progress In Electromagnetics Research Letters*, Vol. 9, 175–181, 2009.

10. Baliarda, C. P. and R. Pous, "Fractal design of multiband and low sidelobes array," *IEEE Trans. Antennas Propagat.*, Vol. 44, No. 5, 730–739, 1996.

11. Haupt, R. L., "Optimized weighting of uniform subarrays of unequal sizes," *IEEE Trans. Antennas Propagat.*, Vol. 55, No. 4, 1207–1210, 2007.

12. Haupt, R. L., "Reducing grating lobes due to subarray amplitude tapering," *IEEE Trans. Antennas Propagat.*, Vol. 33, No. 8, 846–850, 1985.

13. Toso, G., C. Mangenot, and A. G. Roeder, "Sparse and thinned arrays for multiple beam satellite applications," *Proc. of the Second European Conference on Antennas and Propagation (EuCAP 2007)*, 2007.

14. Razavi, A. and K. Forooraghi, "Thinned arrays using pattern search algorithm," *Progress In Electromagnetic Research*, PIER 78, 61–71, 2008.

15. Haupt, R. L., "Thinned arrays using genetic algorithms," *IEEE Trans. Antennas Propagat.*, Vol. 41, No. 2, 993–999, 2003.

16. Lommi, A., L. A. Massa, E. Storti, and A. Trucco, "Sidelobe reduction in sparse linear arrays by genetic algorithms," *Microwave and Optical Technology Letters*, Vol. 32, 194–196, 2002.

17. Vigano, M. C., G. Toso, C. Mangenot, P. Angeletti, and G. Pelosi, "GA optimized thinned hexagonal arrays for satellite applications," *Proc. IEEE Antennas and Propagation International Symposium*, 3165–3168, 2007.

18. Mahanti, G. K., N. Pathak, and P. Mahanti, "Synthesis of thinned linear antenna arrays with fixed sidelobe level using real-coded genetic algorithm," *Progress In Electromagnetic Research*, PIER 75, 319–328, 2007.

19. Kaifas, T., K. Siakavara, D. Babas, G. Miaris, E. Vafiadis, and J. N. Sahalos, "On the design of direct radiating antenna arrays with reduced number of controls for satellite communications," *1st International ICST Conference on Mobile Lightweight Wireless Systems — MOBILIGHT 2009, Proceedings CD*, May 18–20, 2009.

20. Bucci, O. M., T. Isernia, and A. F. Morabito, "A deterministic approach to the synthesis of pencil beams through planar thinned arrays," *Progress In Electromagnetic Research*, PIER 101, 217–230, 2010.

21. Zhang, S., S.-X. Gong, Y. Guan, P.-F. Zhang, and Q. Gong, "A novel IGA-EDSPSO hybrid algorithm for the synthesis of sparse arrays," *Progress In Electromagnetic Research*, PIER 89, 121–134, 2009.

22. Tokan, F. and F. Gunes, "The multi-objective optimization of non-uniform linear phased arrays using the genetic algorithm," *Progress In Electromagnetic Research B*, Vol. 17, 135–151, 2009.

23. Pierro, V., V. Galdi, G. Castaldi, I. M. Pinto, and L. B., Felsen, "Radiation properties of planar antenna arrays based on certain categories of aperiodic tilings," *IEEE Trans. Antennas Propagat.*, Vol. 53, No. 2, 635–644, 2005.

24. Morabito, A. F., T. Isernia, M. G. Labate, M. D'Urso, and O. M. Bucci, "Direct radiating arrays for satellite communications via aperiodic tilings," *Progress In Electromagnetic Research*, PIER 93, 107–124, 2009.

25. Vigano, M. C., G. Toso, G. Caille, C. Mangenot, and I. E. Lager, "Spatial density tapered sunflower antenna array," *Proc. of the 3rd European Conference on Antennas and Propagation (EuCAP 2009)*, 778–782, March 2009.

26. Angeletti, P. and G. Toso, "Aperiodic arrays for space applications: A combined amplitude/density synthesis approach," *Proc. of the 3rd European Conference on Antennas and Propagation (EuCAP 2009)*, 2026–2030, March 2009.

27. Werner, D. H. and T. G. Spence, "Thinning of aperiodic antenna arrays for low side-lobe levels and broadband operation using genetic algorithms," *Proc. IEEE Antennas and Propagation Society International Symposium*, 2059–2062, 2006.

28. Werner, D. H., M. A. Gingrich, and P. L. Werner, "A self-similar radiation pattern synthesis technique for reconfigurable multiband antennas," *IEEE Trans. Antennas Propagat.*, Vol. 51, No. 7, 1486–1498, 2003.

29. Petko, J. S. and D. H. Werner, "The evolution of optimal linear polyfractal arrays using genetic algorithms," *IEEE Trans. Antennas Propagat.*, Vol. 53, No. 11, 3604–3615, 2005.

30. Siakavara, K., E. Vafiadis, and J. N. Sahalos, "On the design of a direct radiating array by using the fractal technique," *Proc. of the 3rd European Conference on Antennas and Propagation*, 1242–1246, Berlin, Germany, March 23–27, 2009.

31. Puente-Baliarda, C., J. Romeu, R. Pous, and A. Cardama, "On the behavior of the Sierpinski multiband fractal antenna," *IEEE Trans. Antennas Propagat.*, Vol. 46, No. 4, 517–524, 1998.

32. Balanis, C. A., *Antenna Theory*, 3rd edition, John Wiley & Sons, New Jersey, 2005.

33. Haupt, R. and S. E. Haupt, *Practical Genetic Algorithms*, John Wiley & Sons, 1998.

34. Rahmat-Samii, Y. and E. Michielssen, *Electromagnetic Optimization by Genetic Algorithms*, Wiley, New York, 1999.

35. Golino, G., "Improved genetic algorithm for the design of optimal antenna division in sub-arrays: A multi-objective genetic algorithm," *Proc. IEEE International Radar Conference*, 629–634, May 2005.

36. Bogard, J. N., D. Werner, and P. L. Werner, "Optimization of Peano-Gosper fractal arrays for broadband performance using genetic algorithms to eliminate grating lobes during scanning," *IEEE Antennas and Propagation Society International Symposium*, Vol. 1B, 755–758, 2005.